

TWO LEVELS HOMOGENEOUS MAGNETIC FLUX DENSITY DISTRIBUTION GENERATED BY PERMANENT MAGNETS ARRANGEMENT

DOC. ING. ALEŠ HÁLA, CSC.

Abstract: At first, the paper shortly deals with magnetic materials used in this application. Then the paper deals with the possibility of creating homogeneous magnetic field by two permanent magnets arrangement. At the end, it deals with possibility of generation of two levels homogeneous magnetic field. The results of computing (2D by FEMM) of some arrangements are discussed. Some results of magnetic circuits arrangement are also discussed.

Key words: Permanent magnet, NdFeB, homogeneous magnetic field, results of computing

INTRODUCTION

There can be found some applications (e.g. in biological experiments) where in the same area have to exist static homogeneous magnetic fields with two different values of magnetic flux density. The discussed arrangement is based on two Watson circuits placed at the defined distance, side by side. The situation is illustrated in Fig. 1.

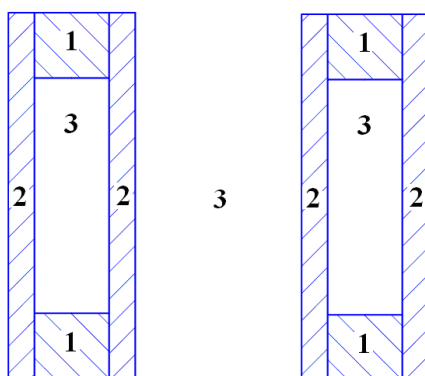


Fig. 1: Magnetic circuit arrangement – Watson circuits side by side. 1- permanent magnet (PM), 2 - magnetically soft sheets, 3 - working area

The length of magnetically soft sheets is 15 cm and their thickness is 1 cm. The distance between Watson circuits is 7.5 cm in our case. Permanent magnets

orientation is the same in both Watson circuits – from the left magnetically soft sheet to the right one.

It is also briefly presented other – material more exacting – Watson circuits arrangement, see Fig. 2. At this arrangement, one Watson circuit is inserted in the other. In this case, permanent magnets magnetization orientation in Watson circuits can be different, see Fig. 2.

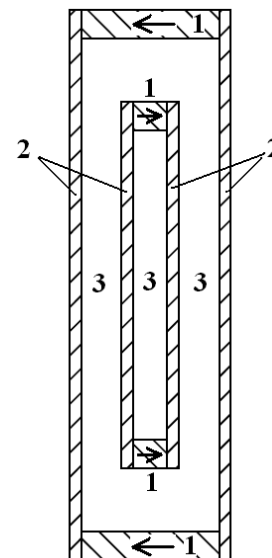


Fig. 2: Magnetic circuit arrangement – Watson circuits one in the other. 1 - permanent magnet (with orientation), 2 - magnetically soft sheets, 3 - working area

1 HARD MAGNETIC MATERIALS MAIN PROPERTIES

Very important property of hard magnetic materials is their energy product $(BH)_{max}$. The development of this property in the last century is given in Fig. 3. It can be seen that higher development is only in NdFeB materials at present time.

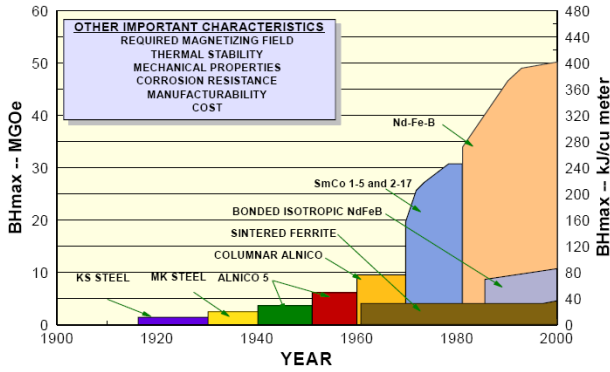


Fig. 3: The development of energy product $(BH)_{max}$ in the last century and other characteristics

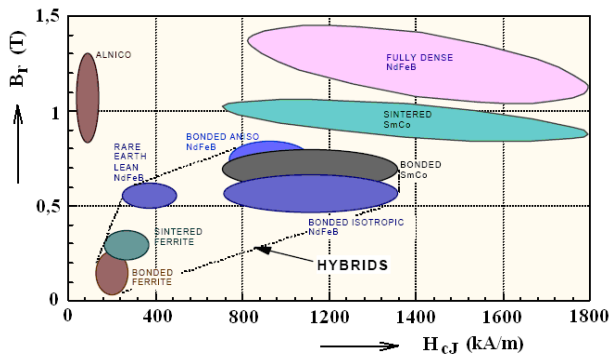


Fig. 4: The relation among internal coercivity H_{cJ} and remanence B_r of different types of permanent magnets

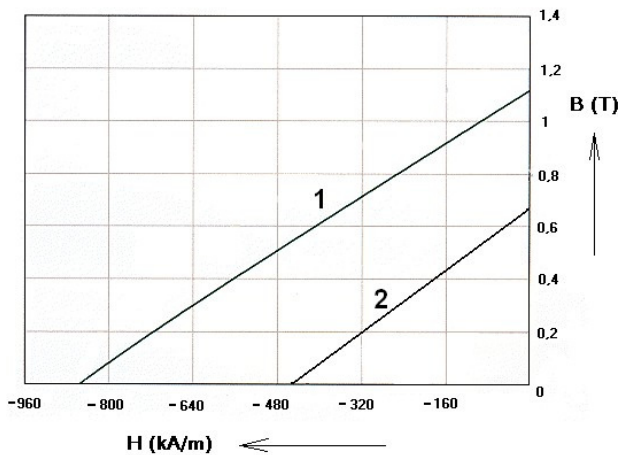


Fig. 5: Typical demagnetization curves: 1- typical NdFeB permanent magnets, 2- typical NdFeB bonded permanent magnets

In Fig.5, there are typical demagnetization curves: 1 typical NdFeB permanent magnets, 2 bonded permanent magnets (NdFeB powder). Both of these materials can be

used in our application. Fully dense permanent magnets used in our application have a little worse demagnetizing characteristic then is shown in typical line 1 (remanence is 0,98 T only).

2 SOME COMPUTING AND MEASUREMENT RESULTS

2.1 Watson circuits side by side – fully dense NdFeB permanent magnets

The used arrangement is shown in Fig. 1. At first, there are discussed some results of computing in the case of use real fully dense permanent NdFeB magnets.

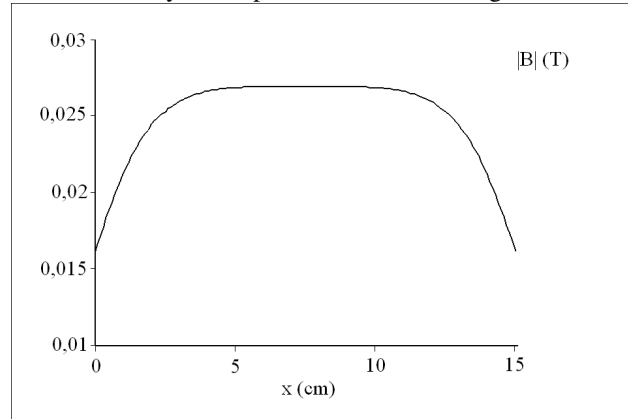


Fig. 6: Magnetic flux density distribution (absolute value) along abscissa $B-B'$ between Watson circuits

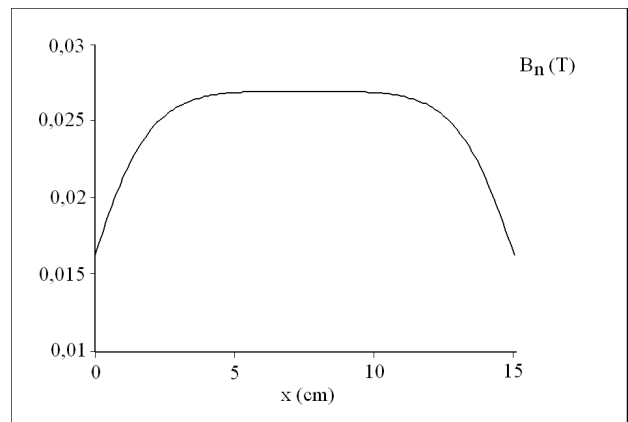


Fig. 7: Magnetic flux density distribution (dominant part) along abscissa $B-B'$ between Watson circuits

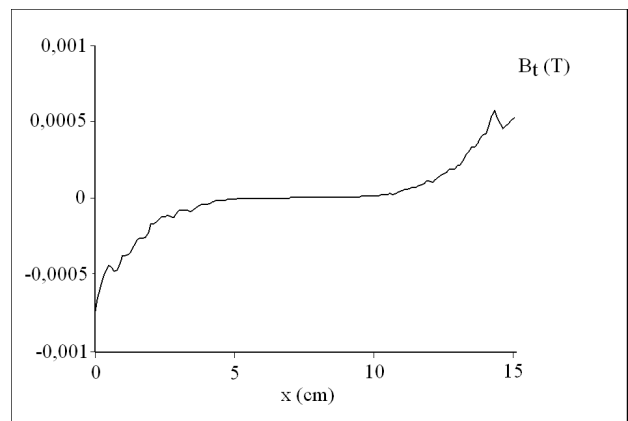


Fig. 8: Magnetic flux density distribution (minor part) along abscissa $B-B'$ between Watson circuits

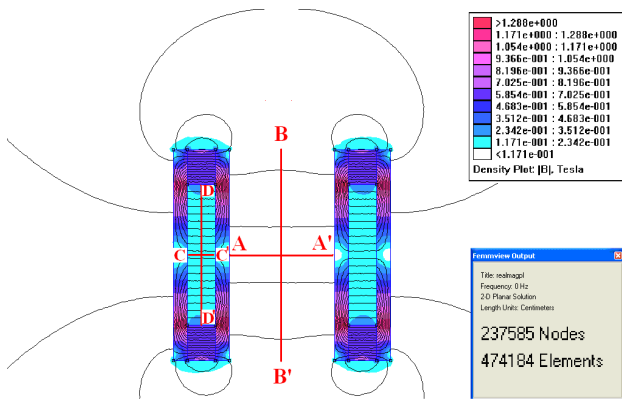


Fig. 9: Map of magnetic flux density absolute value distribution with abscissa A-A', abscissa B-B', abscissa C-C' and abscissa D-D'

The map of magnetic flux density absolute value distribution with abscissas A-A', B-B', C-C' and D-D' is presented in Fig. 9. Absolute value magnetic flux density distributions along these segments are shown in Figs. 10, 6, 13 and 16. Dominant parts magnetic flux density distributions along the same segments are shown in Figs. 11, 7, 14 and 17 and minor parts magnetic flux density distributions along the same segments are shown in Figs. 12, 8, 15 and 18.

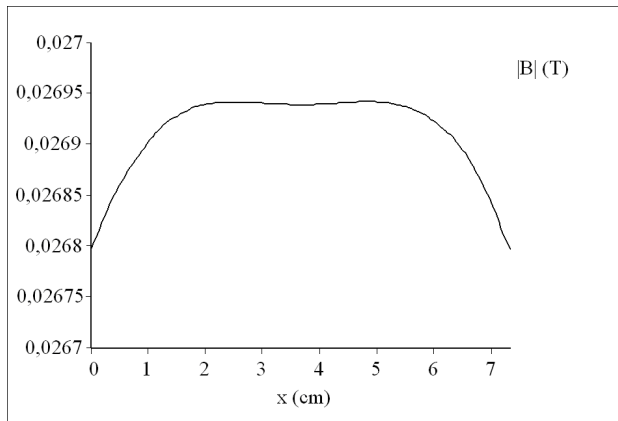


Fig. 10: Magnetic flux density distribution (absolute value) along abscissa A-A' between Watson circuits

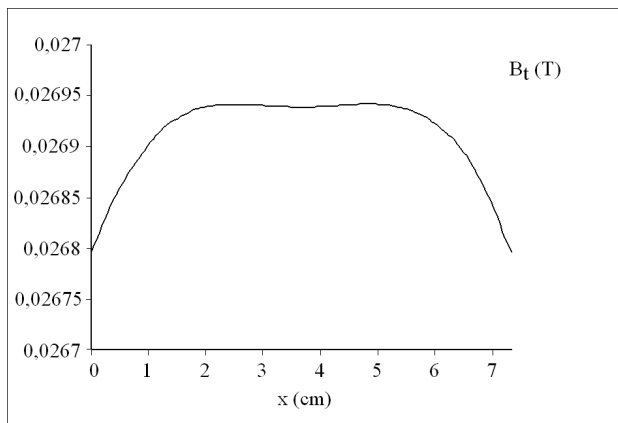


Fig. 11: Magnetic flux density distribution (dominant part) along abscissa A-A' between Watson circuits

It can be seen, that the differences between magnetic flux density B absolute value and dominant part of B are very small. So, only magnetic flux density B absolute values can be presented in the next cases.

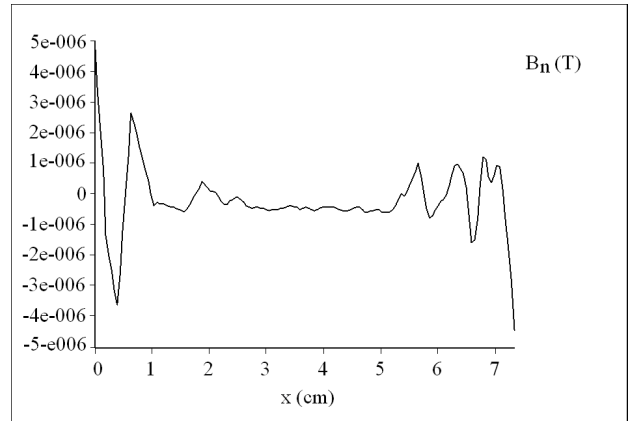


Fig. 12: Magnetic flux density distribution (minor part) along abscissa A-A' between Watson circuits

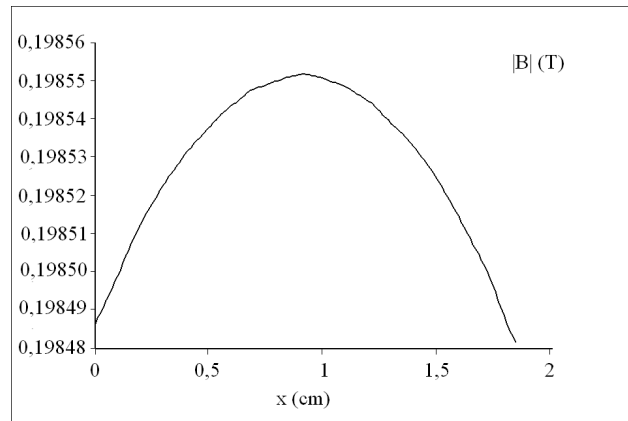


Fig. 13: Magnetic flux density distribution (absolute value) along abscissa C-C' inside left Watson circuit

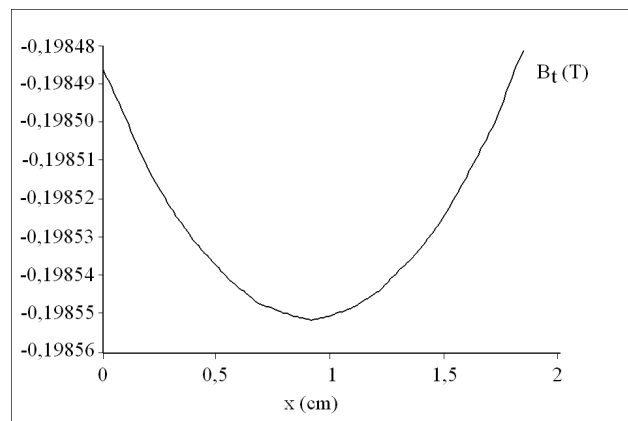


Fig. 14: Magnetic flux density distribution (dominant part) along abscissa C-C' inside left Watson circuit

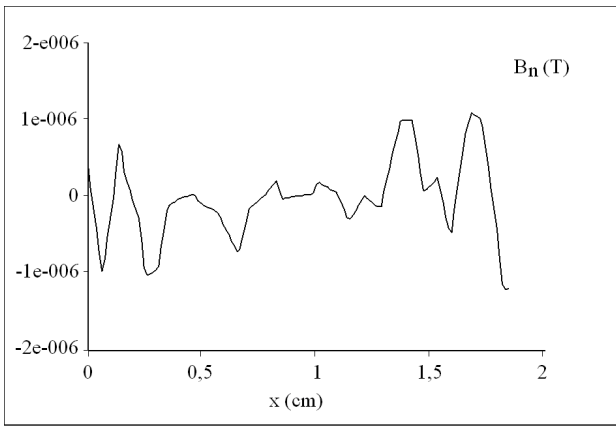


Fig. 15: Magnetic flux density distribution (minor part) along abscissa C-C' inside left Watson circuit

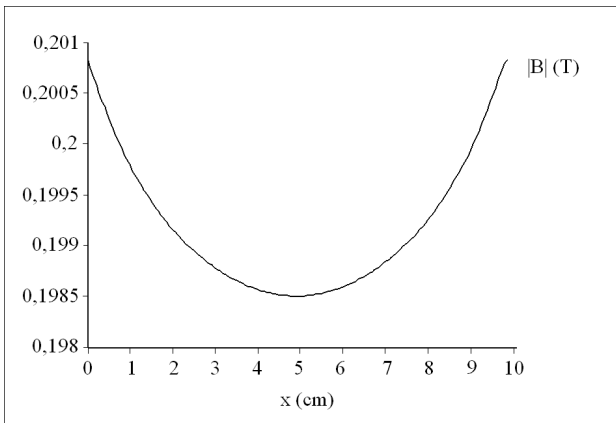


Fig. 16: Magnetic flux density distribution (absolute value) along abscissa D-D' inside left Watson circuit

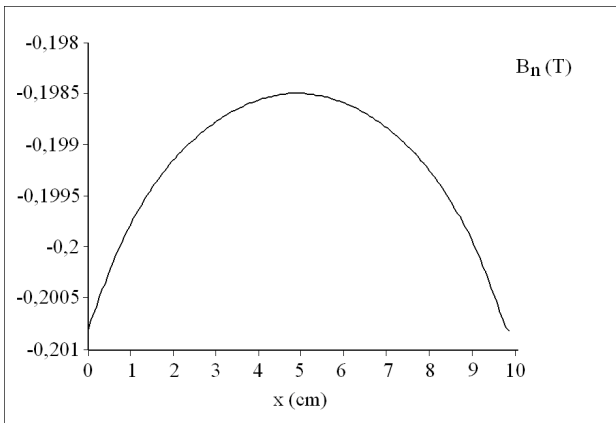


Fig. 17: Magnetic flux density distribution (dominant part) along abscissa D-D' inside left Watson circuit

Some results of magnetic flux density measurements are presented in Fig. 19, Fig. 20 and Fig. 21. It can be said that relatively good conformity with computed results exists. The measurements were realized by magnetic flux density compact measuring instrument Elimag P-21 with Hall probe.

During the measurements, used Hall probe is placed in the holder. The holder is fixed on the modified measuring guide with mm scale (as with vernier calliper).

The movement of Hall probe is realized manually by this measuring guide. The results of measurements have been processed by spreadsheet Excel.

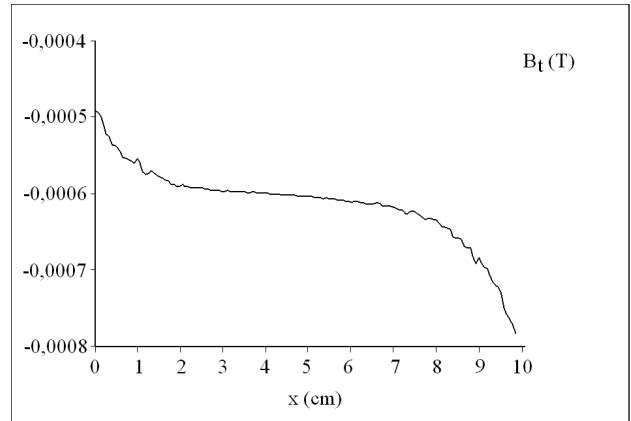


Fig. 18: Magnetic flux density distribution (minor part) along abscissa D-D' inside left Watson circuit

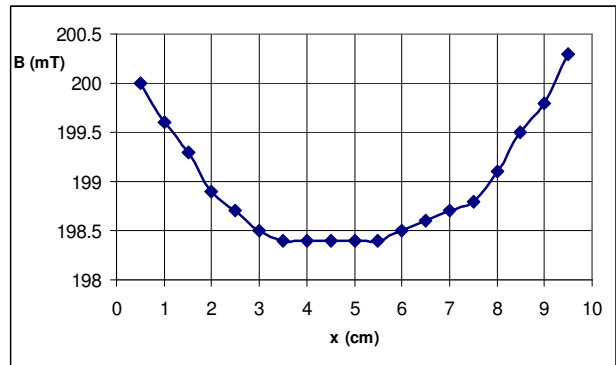


Fig. 19: Measured magnetic flux density distribution (dominant part) along abscissa D-D' inside left Watson circuit

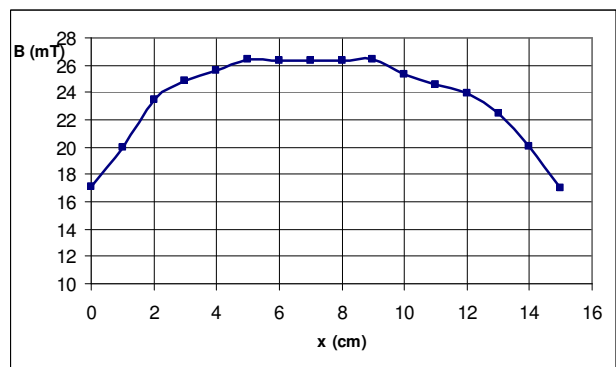


Fig. 20: Measured magnetic flux density distribution (dominant part) along abscissa B-B' between Watson circuits

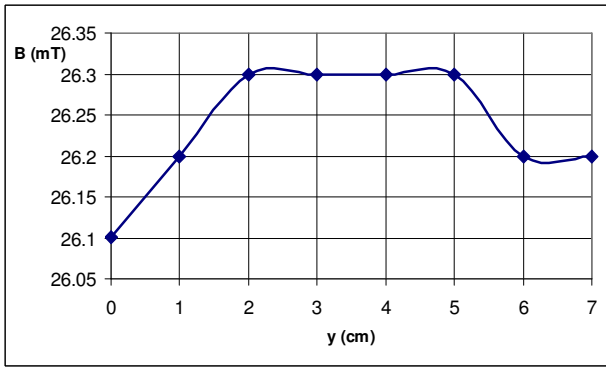


Fig. 21: Measured magnetic flux density distribution (dominant part) along abscissa A-A' between Watson circuits

2.2 Watson circuits side by side – bonded NdFeB permanent magnets

The arrangement and dimensions of Watson circuits are the same as are presented in paragraph 2.1. Bonded permanent magnets maximum energy product is 80kJ/m^3 . Only some computing results along segments A-A', B-B', C-C' and D-D' are presented (see Figs. 23 to 26). The configuration was not practically realized.

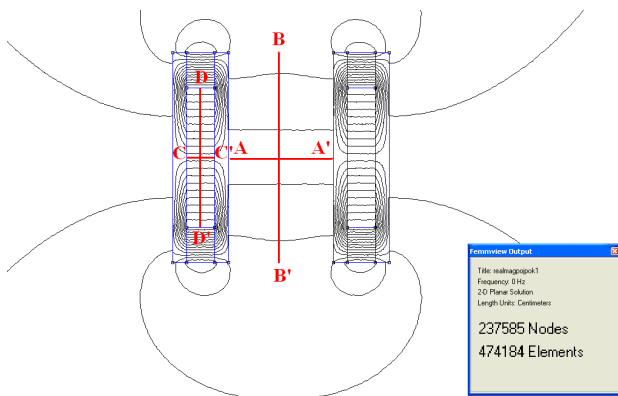


Fig. 22: Magnetic forces lines and abscissa A-A', abscissa B-B', abscissa C-C' and abscissa D-D'.

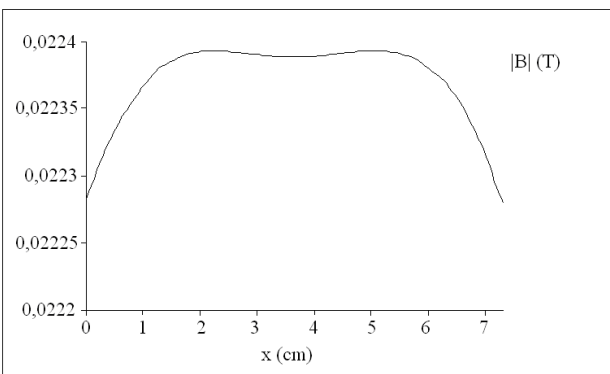


Fig. 23: Magnetic flux density distribution (absolute value) along abscissa A-A' between Watson circuits

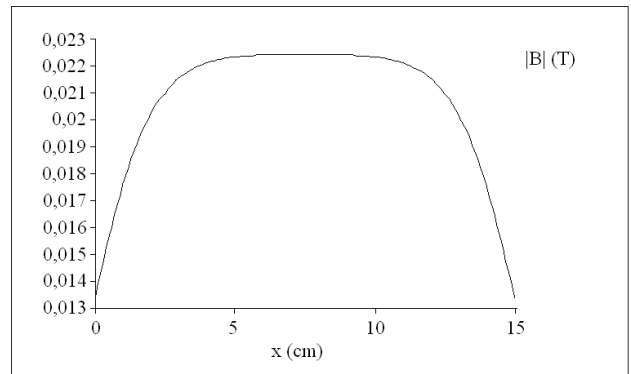


Fig. 24: Magnetic flux density distribution (absolute value) along abscissa B-B' between Watson circuits

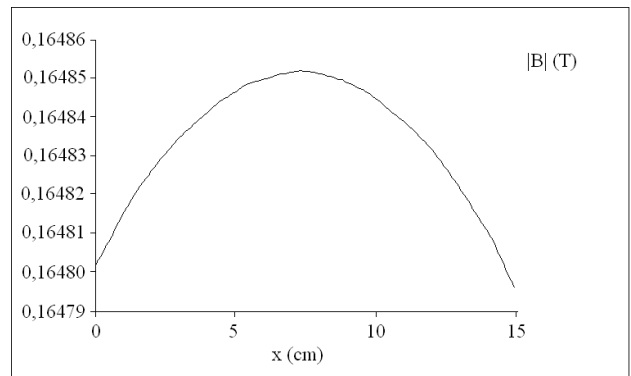


Fig. 25: Magnetic flux density distribution (absolute value) along abscissa C-C' inside left Watson circuit

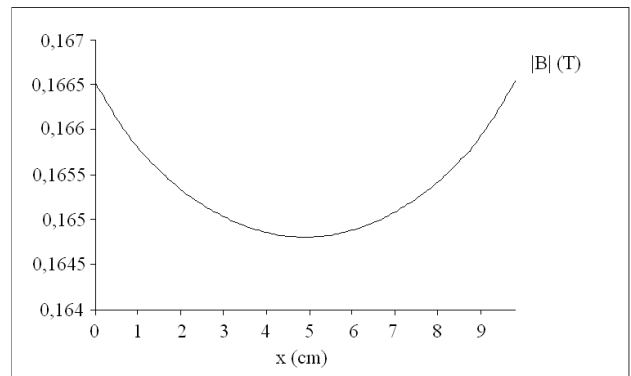


Fig. 26: Magnetic flux density distribution (absolute value) along abscissa D-D' inside left Watson circuit

2.3 Watson circuits one in the other – bonded NdFeB permanent magnets

The configuration of Watson circuits is on a scale sketched in Fig. 2. The thickness of magnetically soft sheets is 1 cm and the length of outer ones is 48 cm. The configuration was not practically realized. As an example, there are presented only two ones (magnetic flux density along the segments A-A' and B-B') from all of the results in Figs. 28 to 30.

The configurations with fully dense NdFeB permanent magnets have been also computed. The results in homogeneity of magnetic flux density distribution are

similar and the magnetic flux density values depend on quality of fully dense permanent magnets.

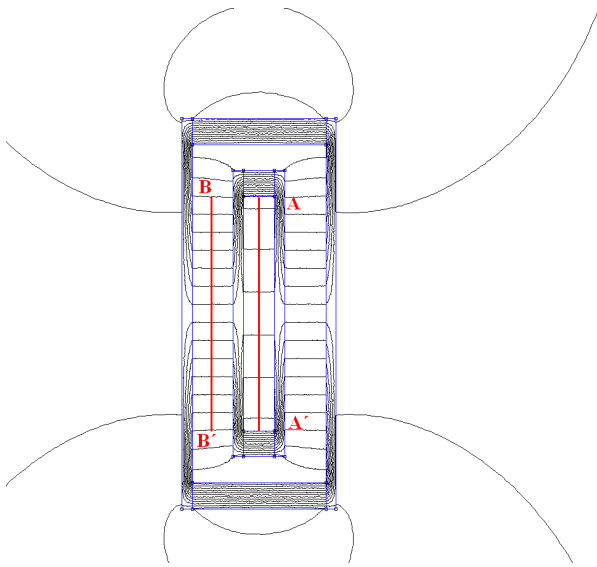


Fig. 27: Magnetic forces lines with the abscissa A-A' and the abscissa B-B'

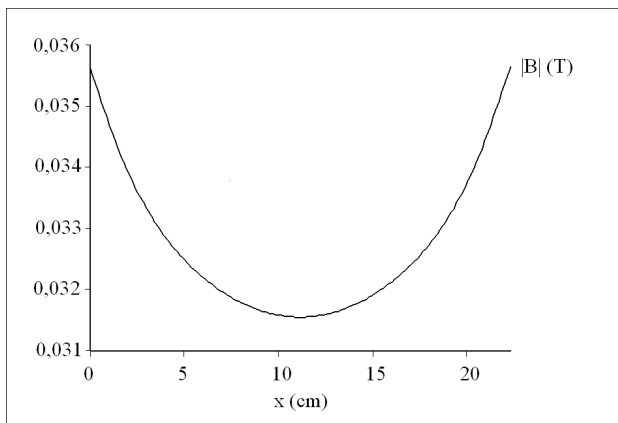


Fig. 28: Magnetic flux density distribution (absolute value) along abscissa A-A'

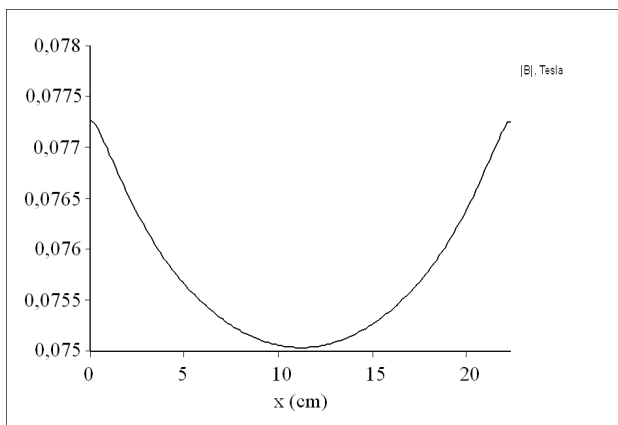


Fig. 29: Magnetic flux density distribution (absolute value) along abscissa B-B'

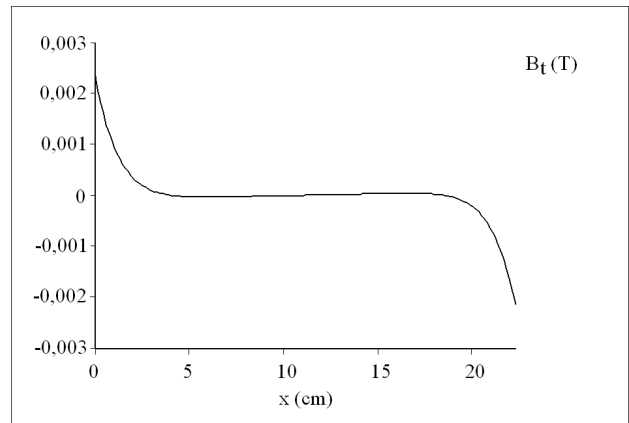


Fig. 30: Magnetic flux density distribution (minor part) along abscissa B-B'

3 CONCLUSIONS

In this paper, there have been shown the arrangements with fully dense NdFeB and bonded NdFeB permanent magnets. There have been presented as well some results of measurements. Magnetic flux density value and its homogeneity one can consider from given figures.

Many other arrangements in both discussed areas (Watson circuits side by side and Watson circuits one in the other) have been computed. There have only been picked out some examples to this paper. But, only one configuration from the first group of circuits was practically tested. All the computing have been realized by 2D programme FEMM (Finite element method magnetics).

At the practical realization of magnetic circuit, it is necessary to take care of heavy forces between permanent magnets. These forces are extremely increased at narrow approach. It is necessary to take high care in handling with permanent magnets by reason of the possibility of the person injury or damage of permanent magnets. NdFeB permanent magnets are very susceptible to corrosion in the case of surface layer damage.

REFERENCES

- [1] Campbell, P.: Permanent Magnet Materials and their Applications. Cambridge University Press, 1994. ISBN 0 521 24996 1.
- [2] <http://www.arnoldmagnetics.com/>
- [3] Hála, A.: The possibility of Helmholtz coils replacement by permanent magnets in the case of homogeneous magnetic fields creation. In Proceedings STO10, Brno, pp. 100-103. UNOB, September 2008. ISBN 978-7231-554-3.
- [4] Meeker, D.: Finite element method magnetics. User manual (www.members.aol.com). October 10, 1999.

Aleš Hála, doc.Ing.CSc, University of Defence, Faculty of Military Technologies, Department of Electrical Engineering, Kounicova 65, 662 10 Brno
email: ales.hala@unob.cz